

Hadron spectroscopy at BESIII

Zhiyong Wang^{*†}

Institute of High Energy Physics, CAS

E-mail: wangzy@ihep.ac.cn

Based on $1310.2 \times 10^6 J/\psi$ events, we study the scalar $f_0(1370)$, $f_0(1500)$, $f_0(1710)$ and pseudoscalar $\eta(1440)/\eta(1405)/\eta(1475)$, $X(p\bar{p})$, and $X(18xx)$. A lot of results are obtained. Some of them are exotic states, or taken as glueball candidates.

XIV International Conference on Heavy Quarks and Leptons (HQL2018)

May 27- June 1, 2018

Yamagata Terrsa, Yamagata, Japan

^{*}Speaker.

[†]

1. Introduction

Glueballs, predicted by QCD, are so exotic from the point of view of naive quark model that their existence will be a direct support of QCD. However, experimental efforts in searching for glueballs are confronted with the difficulty of identifying glueballs unambiguously, even though there are several candidate glueball resonances, such as $f_0(1370)$, $f_0(1500)$, $f_0(1710)$, and $f_J(2220)$, etc. The Lattice QCD predicts that the masses of the lowest-lying glueballs range from 1 to 3 GeV, and suggests that the J/ψ radiative decays be an ideal hunting ground for glueballs. We have studied J/ψ radiative decays and many structures are found. In addition, the exotic study is an interesting topic since the $X(1860)$ has been observed in $J/\psi \rightarrow \gamma p \bar{p}$ in 2003 [1]. A lot of similar exotics are observed with the similar mass. We call these structures $X(18xx)$ states.

2. Study of the scalar meson

2.1 $J/\psi \rightarrow \gamma \eta \eta$

In this analysis, the η meson is detected in its $\gamma\gamma$ decay. Each candidate event is required to have five or six good photons and no charged tracks. Figure 1 (upper-left) shows the distribution of the $\eta\eta$ invariant mass. Many structures are seen.

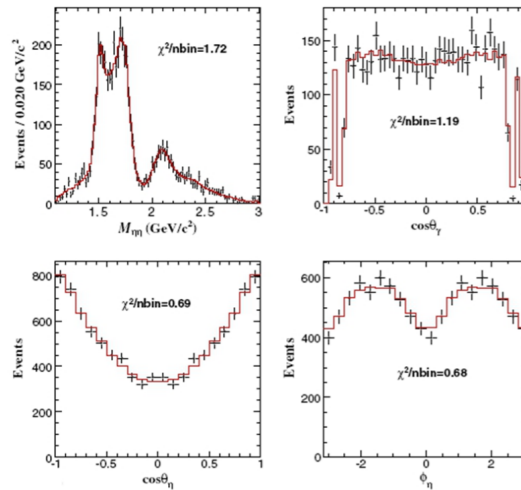


Figure 1: Comparisons between data and PWA fit projections: (a) the invariant mass spectrum of $\eta\eta$, (b)~(c) the polar angle of the radiative photon in the J/ψ rest frame and η in the η helicity frame [the gaps in (b) are due to the photon selection], (d) the azimuthal angle of η in the $\eta\eta$ helicity frame. The black dots with error bars are data with background subtracted, and the solid histograms show the PWA projections.

A partial wave analysis (PWA) is performed to disentangle the structures present in $J/\psi \rightarrow \gamma\eta\eta$ decays. The quasi-two-body decay amplitudes in the sequential decay process $J/\psi \rightarrow \gamma X, X \rightarrow \eta\eta$ are constructed using covariant tensor amplitudes. For an intermediate resonance, the corresponding Breit-Wigner propagator is described by a function:

$$BW(s) = \frac{1}{M^2 - s - iM\Gamma} \quad (2.1)$$

where s is the invariant mass squared of the daughter particles, and M and Γ are the mass and width of the intermediate resonance.

In this analysis, all possible combinations of $0^{++}, 2^{++}, 4^{++}$ resonances are evaluated, and the fitted components with statistical significance larger than 5.0σ are kept as the basic solution. The contribution from $4^{++}[f_4(2050)]$ with a statistical significance of 0.4σ is ignored. There are six resonances, $f_0(1500)$, $f_0(1710)$, $f_0(2100)$, $f'_2(1525)$, $f_2(1810)$, $f_2(2340)$, as well as 0^{++} phase space and $J/\psi \rightarrow \phi\eta$ is included in the basic solution. The dominant scalar are from $f_0(1710)$, $f_0(2100)$. The dominant tensor components are $f'_2(1525)$, $f_2(1810)$ and $f_2(2340)$.

2.2 $J/\psi \rightarrow \gamma\pi^0\pi^0$

In order to be included in the amplitude analysis, an event must have at least five photon candidates and no charged track candidates. Figure 2 shows the invariant mass of $\pi^0\pi^0$. The results of the mass independent amplitude analysis of the $\pi^0\pi^0$ system are obtained from a series of unbinned extended maximum likelihood fits. The amplitudes for radiative J/ψ decays to $\pi^0\pi^0$ are constructed in the radiative multi-pole basis. Any amplitude with total angular momentum greater than zero will have three components (the 0^{++} amplitude has only an E1 component). Thus, three 2^{++} amplitudes, relating to E1, M2, and E3 radiative transitions, are included in the analysis.

The intensities and phase differences for the amplitudes in the fit are presented here as a function of $M_{\pi^0\pi^0}$. Additionally, the intensities and phases for each bin of $M_{\pi^0\pi^0}$ are given in supplemental materials. These results may be combined with those of similar reactions for a more comprehensive study of the light scalar meson spectrum. Finally, the branching fraction of radiative J/ψ decays to $\pi^0\pi^0$ is measured to be $(1.15 \pm 0.05) \times 10^{-3}$, where the error is systematic only and the statistical error is negligible. This is the first measurement of this branching fraction.

3. Pseudoscalar ($0^{-+} - \eta(1440)/\eta(1440)/\eta(1475)$)

The $\eta(1440)$ was observed with $\eta(1440) \rightarrow K\bar{K}\pi$ in $p\bar{p}$ collision. The $\eta(1405)$, $\eta(1475)$ are observed in different decay modes. For example, $\pi^- p$ collision [2], J/ψ radiative decay [3, 4], and $p\bar{p}$ annihilation at rest [5].

Experimentally, $\eta(1440)$ appears as either $\eta(1405)$ or $\eta(1475)$. The former goes to $\eta\pi^+\pi^-$, or to $KK\pi$ through $a_0(980)$ (or directly). The latter goes to $K^*(892)K$ mode. Quark-model predicts two pseudoscalar $\eta(1295)$ and $\eta(1475)$. They are the first radial excitation of η' and η . Someone think $\eta(1405)$ and $\eta(1475)$ are the same state with a mass shift in different modes [6].

In BESII detector, we first observed $\eta(1405)$ and $\eta(1475)$ in J/ψ double radiative decay, $J/\psi \rightarrow \gamma\gamma\rho$ and $J/\psi \rightarrow \gamma\gamma\phi$, respectively [7]. Later, we observed $\eta(1440)$ in $J/\psi \rightarrow \omega(\phi)K\bar{K}\pi$ final states, and the measured mass and width are 1437.6 ± 3.2 MeV/ c^2 and 48.9 ± 9.0 MeV, respectively. In BESIII detector, we observe $\eta(1405)$ in $J/\psi \rightarrow \omega\eta\pi^+\pi^-$ final state [8]. But we just find an evidence of $\eta(1405)$ signal [9]. Figures 3 (left) and (right) show the invariant mass of $\eta\pi^+\pi^-$ in $\omega\eta\pi^+\pi^-$ and $\phi\eta\pi^+\pi^-$ final states, respectively.

We also observe the $\eta(1405)$ signal in the radiative decay of $J/\psi \rightarrow \gamma\pi^+\pi^-\pi^0$ and $J/\psi \rightarrow \gamma\pi^0\pi^0\pi^0$. A single structure around 1.4 GeV/ c^2 in the $\pi^+\pi^-\pi^0$ ($\pi^0\pi^0\pi^0$) mass spectrum is observed, associated with a narrow structure around 980 MeV/ c^2 in the $\pi^+\pi^-$ ($\pi^0\pi^0$) mass spectrum. Figures 4 (a) and (b) show the $\pi^+\pi^-\pi^0$ and $\pi^0\pi^0\pi^0$ mass spectra where $\pi^+\pi^-$ ($\pi^0\pi^0$) is in the

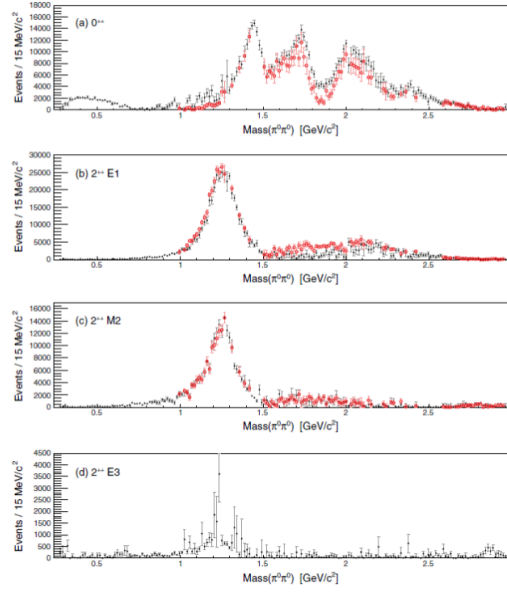


Figure 2: The intensities for the (a) 0^{++} , (b) 2^{+-} E1, (c) 2^{+-} M2, and (d) 2^{+-} E3 amplitudes as a function of $M_{\pi^0\pi^0}$ for the nominal results. The solid black markers show the intensity calculated from one set of solutions, while the open red markers represent its ambiguous partner. Note that the intensity of the 2^{+-} E3 amplitude is redundant for the two ambiguous solutions. Only statistical errors are presented.

$f_0(980)$ mass region ($0.94 \text{ GeV}/c^2 < M_{\pi^+\pi^-}(\pi^0\pi^0) < 1.04 \text{ GeV}/c^2$). In addition to the $\eta(1405)$, there is an enhancement at $1.3 \text{ GeV}/c^2$. A fit is performed to the $\pi^+\pi^-\pi^0$ mass spectrum. The two peaks are parametrized by efficiency corrected Breit-Wigner functions convolved with a Gaussian resolution function. The significance of $\eta(1405)$ in both $\pi^+\pi^-\pi^0$ and $\pi^0\pi^0\pi^0$ final states are all larger than 10σ .

4. $X(18xx)$

4.1 $X(p\bar{p})/X(1860)$ in $J/\psi \rightarrow \gamma p\bar{p}$

Earlier, a strong enhancement was observed in $p\bar{p}$ mass spectrum near $p\bar{p}$ threshold at BES-I [1] and confirmed by CLEO soon. PWA was firstly performed at BESIII [10]. The significance of $X(p\bar{p})$ component is larger than 30σ . The significance for other components is also larger than 5σ . The J^{PC} for this dominant structure is assigned to be 0^\mp . The fitted mass and width are $M = 1832_{-5}^{+19}(\text{stat.})_{-17}^{+18}(\text{syst.}) \pm 19(\text{mode}) \text{ MeV}/c^2$. Figure 5 shows comparisons of the mass and angular distributions between the data and the PWA fit projections. For the spin-parity determination of the $X(p\bar{p})$, the 0^{-+} assignment fit is better than that for 0^{++} or other J^{PC} assignments with statistical significances that are larger than 6.8σ . However, we have not observed the similar structure in $J/\psi \rightarrow \omega p\bar{p}$, and $\phi p\bar{p}$ [11, 12].

4.2 $X(1835)$ in $J/\psi \rightarrow \gamma\pi^+\pi^-\eta'$

A $\pi^+\pi^-\eta'$ resonance, the $X(1835)$, was observed in $J/\psi \rightarrow \gamma\pi^+\pi^-\eta'$ decays with a statistical significance of 7.7σ by the BESII experiment. We re-study this decay mode with $225 \times 10^6 J/\psi$

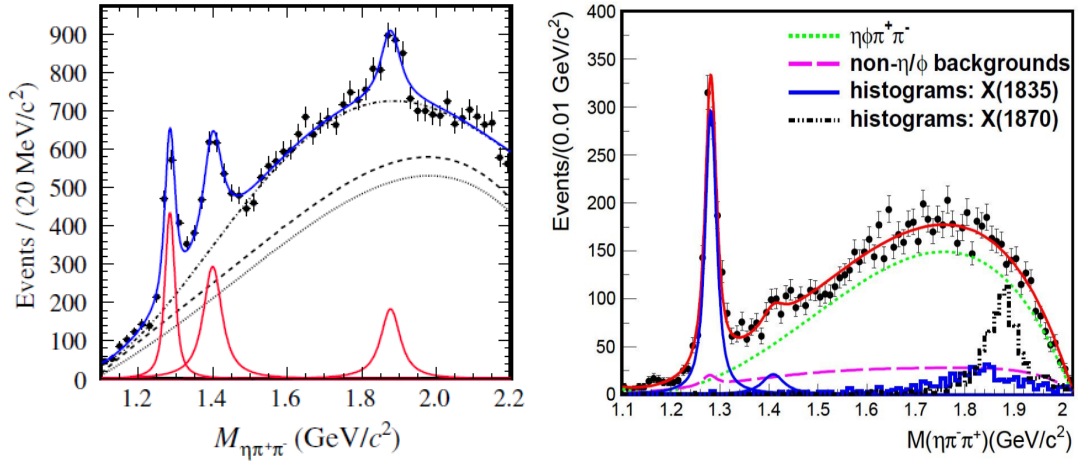


Figure 3: Results of the fit to the $M_{\eta\pi^+\pi^-}$ mass distribution for events with either the $\eta\pi^+$ or $\eta\pi^-$ in the $a_0(980)$ mass window. The dotted curve shows the contribution of non- ω and/or non- $a_0(980)$ background, the dashed line also includes the contribution from $J/\psi \rightarrow b_1(1235)a_0(980)$, and the dot-dashed curve indicates the total background with the non-resonant $J/\psi \rightarrow \omega a_0^\pm(980)\pi^\mp$ included. $\chi^2/\text{d.o.f}$ is 1.27 for this fit.

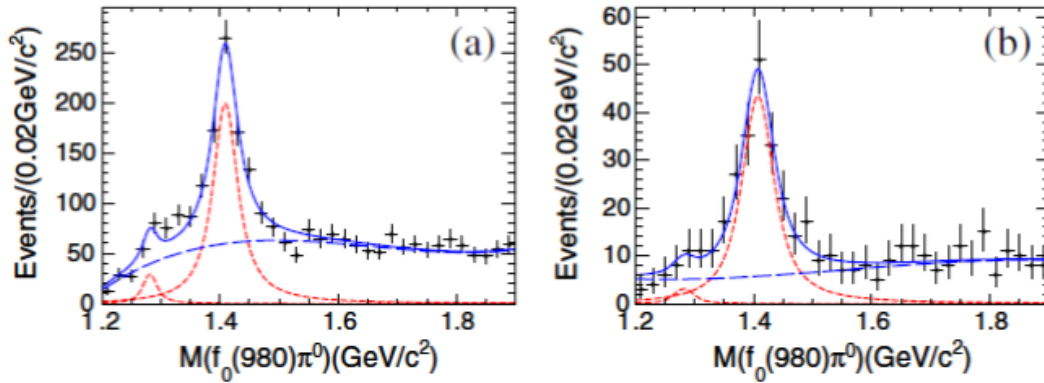


Figure 4: Results of the fit to (a) the $f_0(980) \times (\pi^+\pi^-)\pi^0$ and (b) $f_0(980)(\pi^0\pi^0)\pi^0$ invariant mass spectra. The solid curve is the result of the fit described in the text. The dotted curve is the $f_1(1285)$ and $\eta(1405)$ signal. The dashed curves denote the background polynomial. Angular distributions of the signal include efficiency corrections.

events collected at BESIII detector. Figure 6 (left) shows the $\pi^+\pi^-\eta'$ invariant-mass spectrum for the combined two η' decay modes. Fits to the mass spectra have been made using four efficiency-corrected Breit-Wigner functions convolved with a Gaussian mass resolution plus a non-resonant $\pi^+\pi^-\eta'$ contribution and background representations. Besides the $X(1835)$ is confirmed, three new structures are found. They are $f_1(1510)$, $X(2120)$ and $X(2370)$. We also investigate the angular distribution of $X(1835)$. Figure 6 (right) shows the acceptance-corrected $|\cos\theta_\gamma|$ distribution for the $X(1835)$. The $X(1835)$, which was first observed at BESII, has been confirmed with a statistical significance larger than 20σ . Meanwhile, two resonances, the $X(2120)$ and the $X(2370)$ are observed with statistical significances larger than 7.2σ and 6.4σ , respectively.

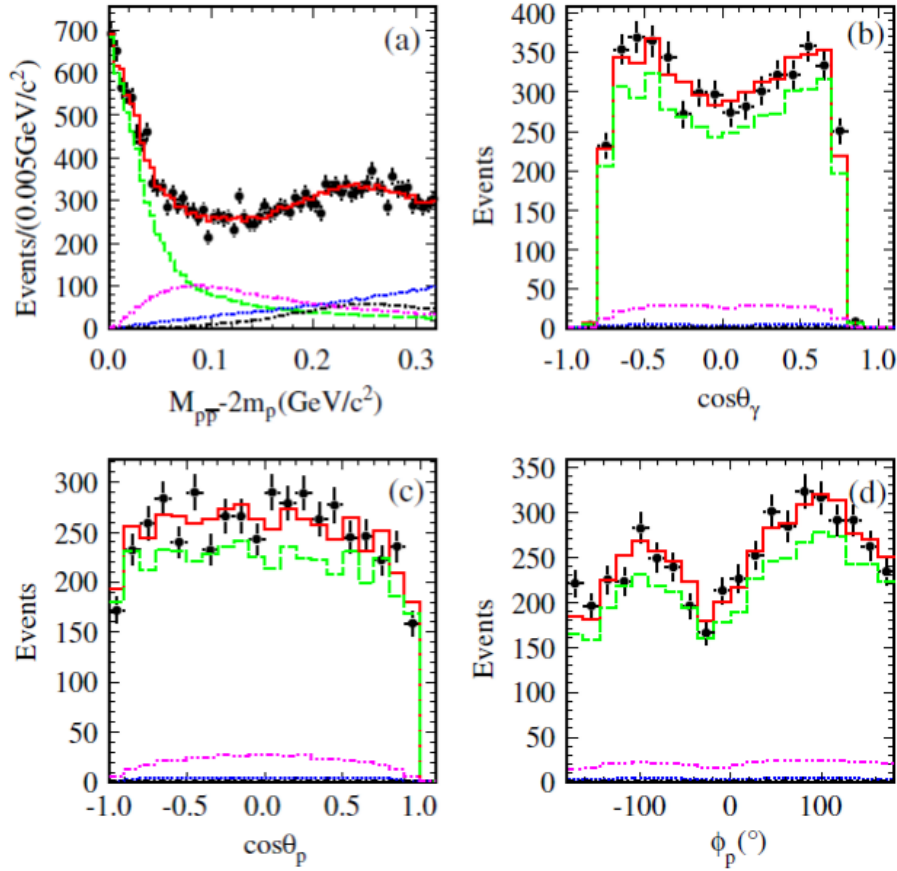


Figure 5: Comparisons between data and PWA fit projection: (a) the $p\bar{p}$ invariant mass; (b)~(d) the polar angle θ_γ of the radiative photon in the J/ψ center of mass system, the polar angle θ_p and the azimuthal angle ϕ_p of the proton in the $p\bar{p}$ center of mass system with $M_{p\bar{p}} - 2m_p < 50$ MeV/c², respectively. Here, the black dots with error bars are data, the solid histograms show the PWA total projection, and the dashed, dotted, dash-dotted, and dash-dot-dotted lines show the contributions of the $X(p\bar{p})$, 0^{++} phase space, $f_0(2100)$ and $f_2(1910)$, respectively.

The masses and widths are measured to be $M = 1835.5 \pm 3.0(stat)^{+5.6}_{-2.1}(syst)$ MeV/c², $\Gamma = 190 \pm 9(stat)^{+38}_{-36}(syst)$ MeV/c² for the $X(1835)$, $M = 2122.4 \pm 6.7(stat)^{+4.7}_{-2.7}(syst)$ MeV/c², $\Gamma = 83 \pm 16(stat)^{+31}_{-11}(syst)$ MeV/c² for the $X(2120)$, and $M = 2376.3 \pm 8.7(stat)^{+3.2}_{-4.3}(syst)$ MeV/c², $\Gamma = 83 \pm 17(stat)^{+44}_{-6}(syst)$ MeV/c² for the $X(2370)$. The production branching fraction for the $X(1835)$ is $\mathcal{B}[J/\psi \rightarrow \gamma X(1835)] \cdot \mathcal{B}(X(1835) \rightarrow \pi^+ \pi^- \eta') = (2.87 \pm 0.09(stat)^{+0.49}_{-0.52}(syst)) \times 10^{-4}$, and the angular distribution of the radiative photon is consistent with a pseudoscalar assignment.

With the much larger J/ψ events collected at BESIII during 2012, we study the $J/\psi \rightarrow \gamma \pi^+ \pi^- \eta'$ process once again and observe a significant abrupt change in the slope of the $\eta' \pi^+ \pi^-$ invariant mass distribution at the proton-antiproton ($p\bar{p}$) mass threshold. We use two models to characterize the $\eta' \pi^+ \pi^-$ line shape around 1.85 GeV/c²: one that explicitly incorporates the opening of a decay threshold in the mass spectrum (Flatté formula), and another that is the coherent sum of two resonant amplitudes. Both fits show almost equally good agreement with data, and suggest the existence of either a broad state around 1.85 GeV/c² with strong couplings to the $p\bar{p}$ final states

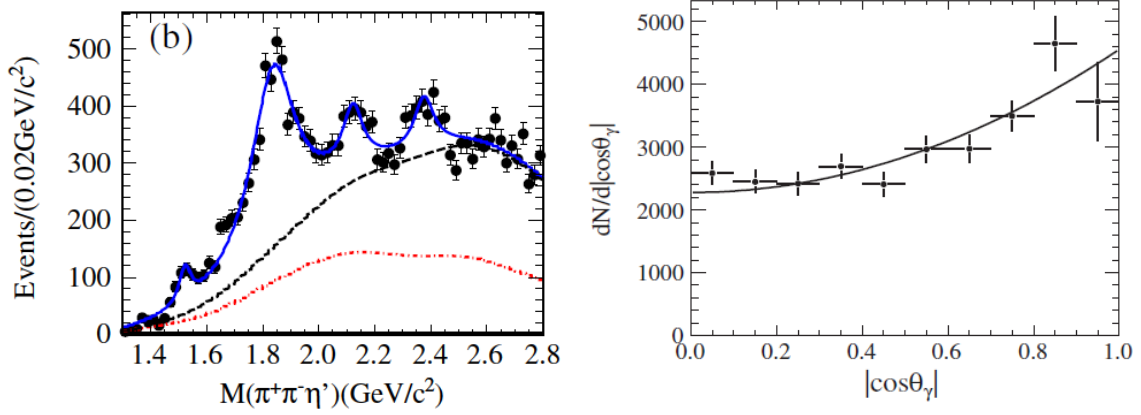


Figure 6: (left) Mass spectrum fitting with four resonances; here, the dash-dotted line is contributions of non- η' events and the background for two η' decay modes, and the dashed line is contributions of the total background and non-resonant $\pi^+\pi^-\eta'$ process. (right) the background-subtracted, acceptance-corrected $|\cos\theta_\gamma|$ distribution of the $X(1835)$ for two η' decay modes for $J/\psi \rightarrow \gamma\pi^+\pi^-\eta'$.

or a narrow state just below the $p\bar{p}$ mass threshold. Although we cannot distinguish between the fits, either one supports the existence of a $p\bar{p}$ moleculelike state or bound state with greater than 7σ significance. Figure 7 shows the fit results.

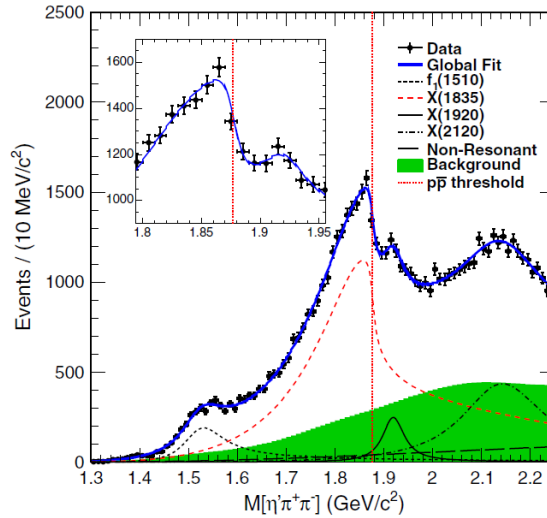


Figure 7: Fit results of using the Flatté formula. The dashed dotted vertical line shows the position of the $p\bar{p}$ mass threshold, the dots with error bars are data, the solid curves are total fit results, the dashed curves are the state around 1.85 GeV/c^2 , the short-dashed curves are the $f_1(1510)$, the dash-dotted curves are the $X(2120)$, the dash-dot-dot-dotted curves are the $X(1920)$, and the long-dashed curves are nonresonant $\eta'\pi^+\pi^-$ fit results; the shaded histograms are background events. The inset shows the data and the global fit between 1.8 and 1.95 GeV/c^2 .

4.3 $X(1835)$ in $J/\psi \rightarrow \gamma K_S^0 K_S^0 \eta'$

We present an observation of the process $J/\psi \rightarrow \gamma X(1835) \rightarrow \gamma K_S^0 K_S^0 \eta'$ at low $K_S^0 K_S^0$ mass

with a statistical significance larger than 12.9σ [13]. In this region of phase space the $K_S^0 K_S^0$ system is dominantly produced through the $f_0(980)$. By performing a partial wave analysis, we determine the spin parity of the $X(1835)$ to be $J^{PC} = 0^{-+}$. The mass and width of the observed $X(1835)$ are $1844 \pm 9(stat)_{-25}^{+16}(syst)$ MeV/ c^2 and $192_{-17}^{+20}(stat)_{-43}^{+62}(syst)$ MeV, respectively, which are consistent with the results obtained by BESIII in the channel $J/\psi \rightarrow \gamma\pi^+\pi^-\eta'$. Figure 8 shows the $K_S^0 K_S^0 \eta'$ mass spectrum with requiring $M_{K_S^0 K_S^0} < 1.1$ GeV/ c^2 . Clear $X(1835)$ signal is seen.

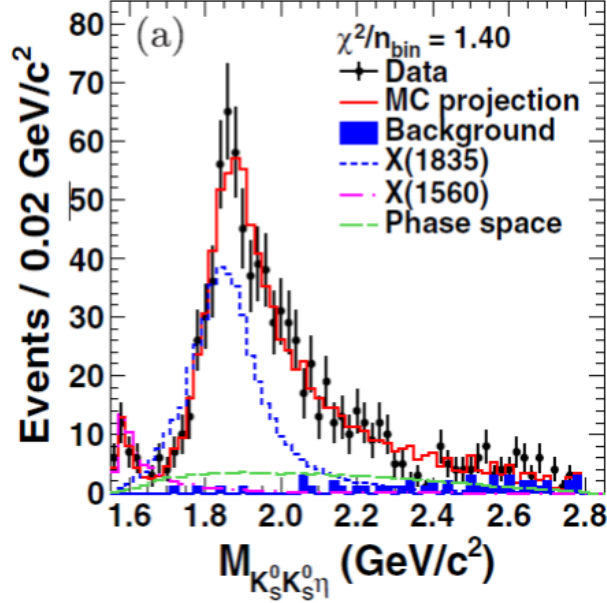


Figure 8: Comparison between data and PWA fit projections for $K_S^0 K_S^0 \eta'$ mass spectrum.

4.4 $X(1870)$ in $J/\psi \rightarrow \omega\eta\pi^+\pi^-$

Besides the $\eta(1405)$ is observed in $\eta\pi^+\pi^-$ mass spectrum, we also observed a new structure, $X(1870)$, at its high mass side, as shown in Fig. 3 (left). The fitted mass and width for $X(1870)$ are $M = 1877.3 \pm 6.3_{-7.4}^{+3.4}$ MeV/ c^2 , $\Gamma = 57 \pm 12_{-4}^{+19}$ MeV/ c^2 [8]. The statistical significance of the $X(1870)$ signal is determined to be 7.2σ . The branching fraction $\mathcal{B}(J/\psi \rightarrow \omega X(1870)) \times \mathcal{B}(X \rightarrow a_0^\pm(980)\pi^\mp) \times \mathcal{B}(a_0^\pm(980) \rightarrow \eta\pi^\pm)$ is measured to be $(1.50 \pm 0.26_{-0.36}^{+0.72}) \times 10^{-4}$. Whether the resonant structure of $X(1870)$ is due to the $X(1835)$, the $X(1870)$, an interference of both, or a new resonance still needs further study such as a partial wave analysis that will be possible with the larger J/ψ data sample.

4.5 $X(1840)$ in $J/\psi \rightarrow \gamma 3(\pi^+\pi^-)$

We studied the decay $J/\psi \rightarrow \gamma 3(\pi^+\pi^-)$. A structure at 1.84 GeV/ c^2 is observed in the $3(\pi^+\pi^-)$ mass spectrum with a statistical significance of 7.6σ [14]. Fitting the structure $X(1840)$ with a modified Breit-Wigner function yields $M = 1842.2 \pm 4.2_{-2.6}^{+7.1}$ MeV/ c^2 . The product branching fraction is determined to be $\mathcal{B}(J/\psi \rightarrow \gamma X(1840)) \times \mathcal{B}(X(1840) \rightarrow 3(\pi^+\pi^-)) = (2.44 \pm 0.36_{-0.74}^{+0.60}) \times 10^{-5}$. Figure 9 shows the fit to $3(\pi^+\pi^-)$ mass spectrum with a Breit-Wigner function modified by the effects of phase-space factor and the detection efficiency. The comparison to the

BESIII results of the masses and widths of the $X(1835)$, $X(p\bar{p})$ [1], $X(1870)$ [8], and $X(1810)$ [15] are displayed in Fig. 9 (right), where the mass of $X(1840)$ is in agreement with those of $X(1835)$ and $X(p\bar{p})$, while its width is significantly different from either of them.

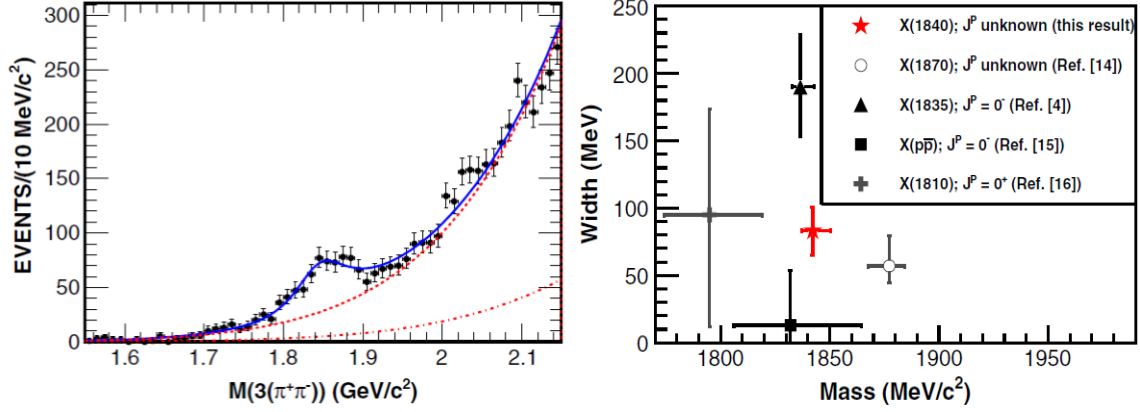


Figure 9: (left) the fit of the mass spectrum of $3(\pi^+\pi^-)$. The dots with error bars are data; the solid line is the fit result. The dashed line represents all the backgrounds, including the background events from $J/\psi \rightarrow \pi^0 3(\pi^+\pi^-)$ (represented by the dash-dotted line, fixed in the fit) and a third-order polynomial representing other backgrounds. (right) Comparisons of observations at BESIII. The error bars include statistical, systematic, and, where applicable, model uncertainties.

References

- [1] J. Z. Bai *et al.* (BES Collaboration), *Phys. Rev. Lett.* **91**, 022001 (2003).
- [2] M. G. Rath *et al.*, *Phys. Rev. D* **40**, 693 (1989).
- [3] Z. Bai *et al.* (The MARK-III Collaboration), *Phys. Rev. Lett.* **65**, 2507 (1990).
- [4] J.-E. Augustin *et al.* (DM2 Collaboration), *Phys. Rev. D* **46**, 1951 (1992).
- [5] A. Bertin *et al.* (OBELIX Collaboration), *Phys. Lett B* **361**, 187 (1995).
- [6] Xiao-Gang Wu, Jia-Jun Wu, Qiang Zhao and Bing-Song Zou, *Phys. Rev. D.* **87**, 014023 (2013).
- [7] J. Z. Bai *et al.* (BES Collaboration), *Phys. Lett. B* **594**, 47 (2004).
- [8] Ablikim *et al.* (BESIII Collaboration), *Phys. Rev. Lett.* **107**, 182001 (2011).
- [9] Ablikim *et al.* (BESIII Collaboration), *Phys. Rev. D.* **91**, 052017 (2011).
- [10] Ablikim *et al.* (BESIII Collaboration), *Phys. Rev. Lett.* **108**, 112003 (2012).
- [11] Ablikim *et al.* (BESIII Collaboration), *Phys. Rev. D.* **87**, 112004 (2013).
- [12] Ablikim *et al.* (BESIII Collaboration), arXiv:1512.08197
- [13] Ablikim *et al.* (BESIII Collaboration), *Phys. Rev. Lett.* **115**, 091803 (2015).
- [14] Ablikim *et al.* (BESIII Collaboration), *Phys. Rev. D.* **88**, 091502 (2013).
- [15] Ablikim *et al.* (BESIII Collaboration), *Phys. Rev. D.* **87**, 032008 (2013).